

## Rarefied-gas heat transfer in micro- and nanoscale Couette flows

W. D. Zhou, B. Liu, S. K. Yu, and W. Hua

*Data Storage Institute, (A\*STAR) Agency for Science, Technology and Research, DSI Building, 5 Engineering Drive 1, Singapore 117608, Singapore*

(Received 22 July 2008; revised manuscript received 6 November 2009; published 26 January 2010)

The physics of the heat conduction and viscous dissipation in rarefied gases is analyzed and discussed. A heat transfer model valid for arbitrary Knudsen numbers, defined as the ratio of the molecular mean free path to the characteristic length of channels, is derived by treating the heat transfer behavior in the slip and transition regimes as an intermediate function of continuum heat transfer model and free molecular heat transfer model. Comparison studies reveal that this model not only shows good agreement with the numerical results based on the direct simulation Monte Carlo method, but also has some unique features that can overcome the deficiencies existing in the previous models. Therefore, this model is capable to study the heat transport phenomena in very dilute gas Couette flows through micro/nanochannels more accurately.

DOI: [10.1103/PhysRevE.81.011204](https://doi.org/10.1103/PhysRevE.81.011204)

PACS number(s): 47.45.-n, 46.55.+d

### I. INTRODUCTION

Microscopic fluidic devices, ranging from surgical endoscopes and micro-electro-mechanical-systems (MEMS) to the slider bearing in the magnetic disk drive, are moving toward a scale unimaginable a decade ago. These devices transport minuscule quantities of gas and liquid along micro- and nanoscale channels. Some thermal assisted techniques are also used in these devices for the various purposes including directing the microscopic flow on a selectively patterned surface [1], inducing a continuous monodirectional rotation in molecular rotors, [2] and increasing magnetic recording density in hard disk drives [3,4]. The flow and heat transfer in such narrow channels usually cannot be dealt with continuum ones because the molecular mean free path is not negligible compared with their characteristic lengths. Accordingly, they must be treated as rarefied-gas flows and heat transfer based on the kinetic theory [5].

The level of rarefaction effect is represented by Knudsen number. Normally, the rarefied flow can be classified into four flow regimes according to their Knudsen number [6]. The flow is considered as a continuum one when  $Kn < 0.01$ . For a large  $Kn > 10$ , the molecular density is low and there are very few collisions between gas molecules. Most collisions occur only at the gap boundaries. This regime is called as free-molecule transport. The continuum flow is governed by the Navier-Stokes equation, whereas the free molecular flow is governed by the collisionless Boltzmann equation. Between the free-molecule regime and the continuum regime, in the range  $10 > Kn > 0.01$ , are the two regimes called the transition and the slip regimes in which both kinds of collisions occur. In today's microscopic fluidic devices, as the minimum spacing continues to decrease to the nanometer level, it is very possible for the systems to operate in a wide range of flow regimes covering the continuum, slip, transition and even free-molecule flow. For example, in the case of magnetic disk drive, the Knudsen number of slider bearing is normally around  $1 \sim 2$ . Further reduction in the slider-disk spacing for a higher recording areal density will drive the Knudsen number even bigger. It is reported that the slider with an inside electrical or optical heater is moving its mini-

um flying height to a level below 2.5 nm [7], which corresponds a Knudsen number well above unity. Figure 1(a) illustrates a thermal nanoactuated slider which uses a heater embedded near its trailing edge. The heat generated by the heater causes the temperature difference across the head-disk interface and also thermal protrusions on air bearing surface to minimize the head-disk spacing. This temperature difference could range from  $20 \sim 30$  °C for an electrical heater to  $300 \sim 400$  °C for an optical heater. Our simulation studies on a thermal nanoactuated slider as shown in Fig. 2 reveal that the Knudsen number is estimated as 11 on its trailing edge whereas it is smaller than 0.01 on some other places. Therefore, it is necessary to study heat and momentum transport in the entire Knudsen regime.

Some attempts have already been made in this area. However, it seems that most previous works rely on atomic-based simulation methods such as molecular dynamics (MD) [8–10] and the direct simulation Monte Carlo (DSMC) [11,12]. Although these methods have been successfully applied for probing the microscopic behavior of gas and liquid at interfaces or clearances, they usually require complicated statistics calculation and high CPU cost, which are not easy to be used in the engineering field. To solve this problem, Zhang and Bogoy [13] derived a heat transfer model based on

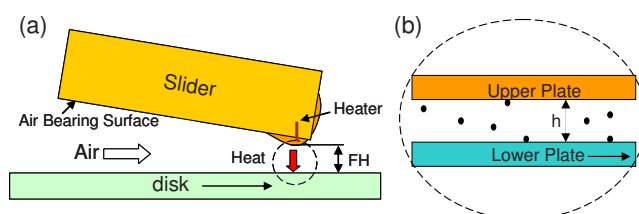


FIG. 1. (Color online) Left (a): an air bearing slider with thermal actuator. The heat generated by the heater causes the pole-tip protrusion to reduce the slider flying height (FH). However, most heat will dissipate from the slider to the rotating disk due to cooling effect of air bearings. Right (b): enlarged view of pole-tip protrusion area where we can simplify as two parallel plates with a spacing of  $h$  when deriving the equation for free molecular heat transfer. The upper plate is stationary and the lower plate is moving at a constant velocity  $U$ .

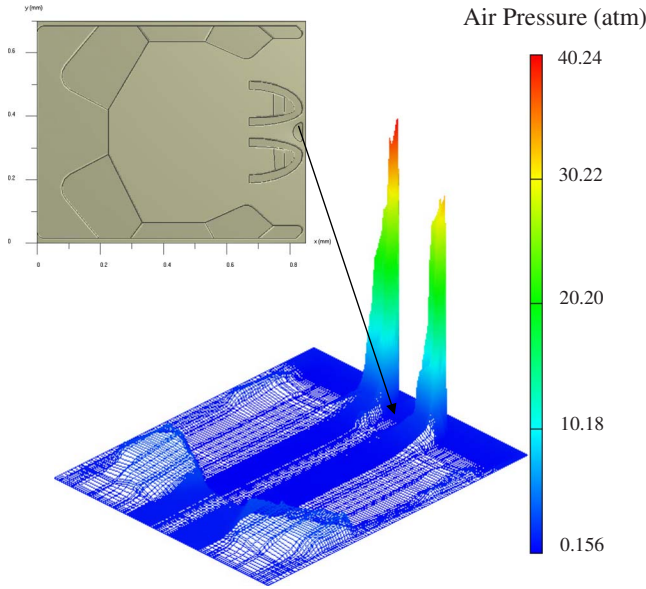


FIG. 2. (Color online) Top: air bearing slider with thermal protrusion on a separate small trailing pad to house the head element. Bottom: the pressure distribution on air bearing surface. The flying height and air pressure on the trailing pad is around 3.7 nm and 1.6 atmospheres, respectively, at a heating power of 20 mW.

the continuum equations such as the Navier-Stokes equations and energy equation with the appropriate modifications on the boundary conditions. Ju [14] used the similar temperature jump theory to solve the heat conduction but calculated the viscous dissipation in microscale Couette flows based on an approximate solution to the Boltzmann transport equation. While these models are being widely used in solving heat transport problems in the air bearing sliders [3,4,13–16] of disk drives, the physical justification of its applicability to high Knudsen number regime is not clear as the continuum description is valid only as long as the Knudsen number is sufficiently small [8]. A large Knudsen number will lead to the failure of continuum assumptions to gas, even though the simulation is corrected by using the appropriate modifications on the continuity equations [17]. Recently, Shen and Chen [18] developed a generalized heat transfer model based on the linearized Boltzmann equation. A comparison study among various heat transfer models was also made and a reasonable agreement with Ju’s model was found. Although Shen’s model is claimed to be more accurate in predicting the heat flux, its accuracy depends on numerical solution of complex integral equations with respect to the molecule velocities and thus it is not easy to be used in the engineering field too. In this article, we will use a totally different method to derive a heat transfer model, which could be valid for arbitrary Knudsen numbers. We will consider the heat conduction and viscous dissipation in free-molecule and continuum regimes, respectively, and use an approximate method to calculate the heat conduction and viscous dissipation in the slip and transition flow regions. Although our derivations are illustrated with a nanochannel similar to the head-disk interface of a disk drive, the heat transport in micro/nanochannels should be a universal problem which may occur in many other microscopic fluidic devices as well.

## II. DERIVATION OF A HEAT TRANSFER MODEL

### A. Heat conduction

The heat transfer in the free-molecule flow regime at head-disk interface can be simplified as the one-dimensional heat transfer between two stationary plates as shown in Fig. 1. The heat dissipation caused by moving the plate will be considered later. Assuming the effect of intermolecular collisions is negligible and also diffuse reflection with thermal accommodation coefficients of  $\alpha_1$  and  $\alpha_2$  at the upper and lower plates, respectively, we can obtain the following expressions from the definition of thermal accommodation coefficients as

$$\text{heat flux for lower plate: } q_1 - q_2 = \alpha_2(q_1 - q_{w,2}), \quad (1a)$$

$$\text{heat flux for upper plate: } q_2 - q_1 = \alpha_1(q_2 - q_{w,1}), \quad (1b)$$

combining (1a) and (1b):

$$q_1 - q_2 = \frac{\alpha_1 \alpha_2}{\alpha_1 + \alpha_2 - \alpha_1 \alpha_2} (q_{w,1} - q_{w,2}) = \alpha (q_{w,1} - q_{w,2}), \quad (1c)$$

where  $q_1$  and  $q_2$  are the incident and reflected energy fluxes for the lower plate which are also the reflected and incident energy flux for the upper plate,  $\alpha$  is the overall accommodation coefficient between two plates,  $q_{w,1}$  and  $q_{w,2}$  are the reflected energy fluxes if all incoming molecules had been carried away with energy fluxes corresponding to the wall temperature  $T_1$  at the upper plate and  $T_2$  at the lower plate, respectively.

For an equilibrium nonreacting gas in Maxwellian distribution,  $q_{w,1}$  and  $q_{w,2}$  are the sum of translational energy flux and internal energy flux, which can be obtained by solving collisionless Boltzmann equation [19] as

$$q_{w,i} = \frac{\gamma + 1}{2(\gamma - 1)} m R T_i N_{w,i}, \quad i = 1, 2, \quad (2)$$

where  $m$  is molecular mass,  $R$  is the molar gas constant,  $\gamma$  is the ratio of the specific heat, and  $N_{w,i}$  is the number flux (per unit area per unit time) of diffusely reflected molecules from the upper and lower plates, which equals to the effusion of molecules from a fictitious equilibrium gas when no accumulation of gas molecules on the surface is assumed, that is

$$N_w = N_{w,1} = N_{w,2} = n \sqrt{\frac{RT}{2\pi}}, \quad (3)$$

where  $n$  is number density,  $T$  is the absolute temperature of gas.

Combining Eqs. (1a)–(1c), (2), and (3), the resulting net free-molecule heat flux can be written as

$$q_{FM} = q_2 - q_1 = -\alpha \frac{\gamma + 1}{\gamma - 1} n m \sqrt{\frac{RT}{2\pi}} (T_1 - T_2). \quad (4)$$

The gas temperature  $T$  in Eq. (4) can be expressed by the plate temperature. Assuming the reflected molecules from the upper and lower plates are in Maxwellian distribution and their temperatures are  $T_{r,1}$  and  $T_{r,2}$ , respectively, we can derive the relation for gas temperature as

$$\sqrt{T} = \frac{2\sqrt{T_{r,1}T_{r,2}}}{\sqrt{T_{r,1}} + \sqrt{T_{r,2}}}, \quad (5)$$

where  $T_{r,1} = [\alpha_1 T_1 + \alpha_2(1 - \alpha_1)T_2] / (\alpha_1 + \alpha_2 - \alpha_1\alpha_2)$  and  $T_{r,2} = [\alpha_2 T_2 + \alpha_1(1 - \alpha_2)T_1] / (\alpha_1 + \alpha_2 - \alpha_1\alpha_2)$ .

The relation in Eq. (4) can also be rewritten by treating the gas particle like a hard sphere and thus, setting  $\rho = nm = (\mu/\lambda)(\pi/2RT)^{1/2}$ ,  $(\gamma - 1) = \gamma R/c_p$ ,  $c_p = k \text{Pr}/\mu$ . This gives

$$q_{FM} = -\alpha \frac{\gamma + 1}{\gamma} \frac{k \text{Pr}}{4\lambda} (T_1 - T_2), \quad (6)$$

where  $k$  is the thermal conductivity of gas,  $c_p$  is the specific heat capacity,  $\lambda$  is the mean free path,  $\mu$  is viscosity of a gas, and  $\text{Pr}$  is Prandtl number.

The continuum heat conduction between the plates is based on Fourier's law and can be written as

$$q_c = -k(dT/dz) = -k(T_1 - T_2)/h. \quad (7)$$

From Eqs. (6) and (7), we can see that the mechanism for free-molecule and continuum heat conduction is different. The heat conduction in free-molecule regime is proportional to the gas density and is independent of the spacing between the walls, whereas the heat conduction in continuum flow regime is inversely proportional to the plate spacing and independent of the density. The ratio of the continuum to the free-molecule heat conduction is found to be proportional to the Knudsen number of the flow, that is

$$\frac{q_c}{q_{FM}} = \frac{4\gamma}{(\gamma + 1)\alpha \text{Pr}} \frac{\lambda}{h} \propto \frac{\lambda}{h} \propto (\text{Kn}). \quad (8)$$

For the transition and slip regimes, which lie in the range  $10 > \text{Kn} > 0.01$ , the heat conduction can be approximated as an intermediate function of the asymptotic processes of continuum heat conduction and free molecular heat conduction. This approach has been shown to agree well with experimental data for heat transfer through rarefied argon and helium [20]. The formula based on this approach is given approximately by Springer [21] and Tien and Cunningham [22] as

$$\frac{q}{q_{FM}} = \left(1 + \frac{q_{FM}}{q_c}\right)^{-1} = \left(1 + \frac{c}{\text{Kn}}\right)^{-1}, \quad \frac{q}{q_{FM}} + \frac{q}{q_c} = 1, \quad (9)$$

where  $c = \alpha(\gamma + 1)\text{Pr}/4\gamma$  is a constant.

After rearranging Eq. (9) with Eq. (6), we can obtain a heat conduction model valid for arbitrary Knudsen number as

$$q = -k \frac{T_1 - T_2}{h + 4\gamma\lambda/\alpha(\gamma + 1)\text{Pr}}. \quad (10)$$

### B. Viscous dissipation

The free-molecule heat transfer can also be extended to Couette flow by giving the lower plate a velocity  $U$  and

keeping the upper plate stationary, as shown in Fig. 1. The number fluxes and the normal momentum flux are not affected by this velocity. Assuming the complete momentum accommodation at both plates, the viscous dissipation in the fluid can be derived as [19]

$$q_{FM\_viscous} = \rho U^2 (RT/8\pi)^{1/2}, \quad (11)$$

where  $\rho$  is the gas density.

However, this diffusive model is normally invalid for the interactions with very smooth and clean surfaces as those of the head and disk in the drive. In such a case, the velocity of reflected gas molecule on the upper plate will not be zero. If we set its velocity as  $cU$ , then the velocity of reflected gas molecule on the lower plate will be  $(1 - c)U$  according to its symmetry distribution. In the reflected gas molecules, some fraction  $\sigma$  of molecules are reflected diffusely with the disk velocity  $U$  while the remainder are reflected specularly with the velocity  $cU$ . Accordingly, we can have the following relation:

$$\sigma U + (1 - \sigma)cU = (1 - c)U \quad (12)$$

to solve for

$$c = \frac{1 - \sigma}{2 - \sigma}$$

$$U_L = (1 - c)U = \frac{1}{2 - \sigma}U. \quad (13)$$

After obtaining the gas molecular velocity on the lower plate, we can rewrite Eq. (11) by considering the momentum accommodation coefficient on the plate

$$q_{FM\_viscous} = \frac{\sigma}{2 - \sigma} \rho U^2 (RT/8\pi)^{1/2}. \quad (14)$$

The viscous dissipation for continuous Couette flow can be written as

$$q_{c\_viscous} = \mu U^2/2h. \quad (15)$$

The viscous dissipation in the transition and slip regimes can also be approximated by using the same approach and can be written as

$$\frac{q_{viscous}}{q_{FM\_viscous}} = \left(1 + \frac{q_{FM\_viscous}}{q_{c\_viscous}}\right)^{-1} = \left(1 + \frac{\sigma}{2 - \sigma} \frac{h}{2\lambda}\right)^{-1}. \quad (16)$$

Now, we can derive a general expression for viscous dissipation that considers the effect of the momentum accommodation coefficient on the plate surfaces as

$$q_{viscous} = \frac{1}{8} \rho U^2 \left(\frac{8RT}{\pi}\right)^{1/2} \frac{1}{a + h/2\lambda}, \quad (17)$$

where  $a = (2 - \sigma)/\sigma$ .

### III. MODEL COMPARISON AND VALIDATION

#### A. DSMC method

To validate the models proposed in the paper, DSMC method is used simultaneously for the numerical simulation of micro/nanoscale Couette flows. A DSMC code is developed based on the method proposed by Bird [19]. DSMC method is a direct particle simulation method based on kinetic theory. It models the flow as a collection of discrete particles with various positions, velocities, and energies. Each simulated particle represents a number of real molecules which have the same properties. During the simulation, the molecular motions and the intermolecular collisions are uncoupled over small time intervals that are less than the mean collision time. The macroscopic quantities, such as velocities, densities, and temperatures are obtained using the statistical methods by sampling the microscopic quantities of all the particles in the computational domain. A good introduction of this method is given in the book by Bird [19].

In DSMC simulations, we divided rarefied-gas transfer problems into two separate ones: (1) heat conduction between two parallel plates caused by various plate temperatures; and (2) viscous dissipation caused by the movement of lower plate. The gap between the plates is filled with rarefied-argon gas. The argon gas is chosen as a working fluid because it is a simple monatomic molecule gas with zero internal degree of freedom. Under ambient conditions, the number density of argon is  $n_0 = P_0 / (kT_0) = 2.6883 \times 10^{25} \text{ m}^{-3}$  (here, the Boltzmann constant  $k = 1.380 622 \times 10^{-23}$ ), the molecular mass is  $6.63 \times 10^{-26} \text{ kg}$ , and the mean free path is 62 nm [19]. The Knudsen number  $Kn$  is varied so that we could cover the flow range from the continuum to the free molecular limit. This is done by changing the distance between the plates. For example, when the height at the plates is fixed at 6.2  $\mu\text{m}$ , 62, and 6.2 nm, respectively, the resulting  $Kn$  number will be  $10^{-2}$ , 1, and 10, accordingly.

There are four parameters to control numerical error in the DSMC method [19]: the cell size, the sample size, the number of simulation particles per cell, and the time step. Bird [19] recommended that the cells should be no larger than one third of the local mean free path and contain at least twenty particles, and that the time step should be kept below one fourth of the local mean collision time. In our simulation, we select these parameters more carefully so that the numerical errors can be reduced to negligible levels. The gap between the plates is divided into 200 cells and each cell into 10 subcells. A test study using 400 uniform cells is also performed and the numerical errors in predicting heat flux and viscous dissipation rate are found to be below 1%. A unified number of 100 000 particles are set initially. The simulation particle number in each cell is around 50, which could ensure the statistical accuracy of the DSMC computation. The time step is chosen in such a way that the molecules moves about one third of the cell dimension at each time step, which is also much less than the mean collision time. To minimize the statistical error, a large number of approximately  $10^7$  samples were taken. A test study using  $10^8$  samples was performed and the numerical errors are found to

be less than 0.5%. So this sample size should be sufficient for our current study. The variable hard sphere (VHS) molecule with a diameter of  $d = 4.17 \times 10^{-10} \text{ m}$  is used to compute collision rates between the argon molecules. The VHS model is adopted here as it is more adequate than the hard sphere model for the modeling of real gas flows. The VHS model would not only reproduce the coefficient of viscosity, but also the realistic temperature exponent of the coefficient of viscosity [19].

There are two types of boundary conditions commonly used in the DSMC method, the specular and diffusive reflection. In a specular reflection, the normal velocity is reversed, the tangential velocity is retained and the energy preserved. Diffusive reflection is a more realistic boundary condition since it allows for transfer of both energy and tangential momentum. However, for the interactions with very smooth and clean surfaces as those of heads and disks in the drives, the above two idealized model become invalid. Therefore, we propose to apply Maxwell model to study the effect of accommodation coefficient on the heat transfer between the plates. In this model, it is assumed that a fraction  $\alpha$  molecule is diffusively reflected with accommodation coefficient  $\alpha = 1$  and the rest are specularly reflected with accommodation coefficient  $\alpha = 0$ . Then, the reflected energy flux  $q_r$  will be

$$q_r = \alpha q_w + (1 - \alpha) q_i, \quad (18)$$

where  $q_i$  is incident energy flux and  $q_w$  is the energy flux that would be carried away in diffuse reflection with the wall temperature.

In order to validate our DSMC code, we compare the temperature and velocity profiles of the present DSMC method with the DSMC results computed by Gallis *et al.* [23], as shown in Fig. 3. In this simulation, the upper and lower walls have temperatures of 308.15 and 238.15 K and tangential velocities of 50 and  $-50 \text{ m/s}$ , respectively. The other simulation conditions are also set similar to the ones provided by Gallis *et al.* [23]. The results of the current DSMC simulation and those of Gallis *et al.* [23] are in good agreement. The heat flux and shear-stress Knudsen numbers corresponding to these conditions are also found to be exactly the same. Therefore, our DSMC code can be well validated.

#### B. Heat conduction

We now compare our heat conduction expression in Eq. (10) with the ones from the previous models. In these models, the heat conduction terms can be written in a similar style as

$$q = -k \frac{T_1 - T_2}{h + 4\gamma\lambda\alpha(\alpha_1, \alpha_2)/(\gamma + 1)\text{Pr}}, \quad (19)$$

where  $\alpha(\alpha_1, \alpha_2) = 1$ , in Ju's model;

$$\alpha(\alpha_1, \alpha_2) = (2 - \alpha_E)/\alpha_E, \text{ in Zhang's model;}$$

$\alpha(\alpha_1, \alpha_2) = (\alpha_1 + \alpha_2 - \alpha_1\alpha_2)/\alpha_1\alpha_2$ , in the proposed model.

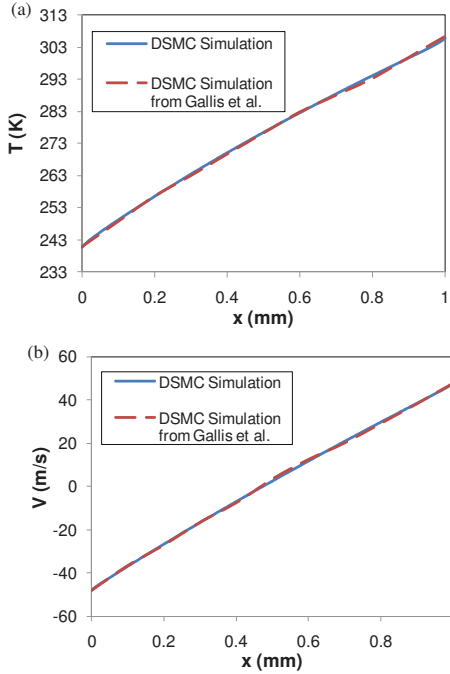


FIG. 3. (Color online) Comparison of the present DSMC method with the DSMC results computed by Gallis *et al.* (Ref. [23]) in (a) temperature and (b) velocity profiles.

From inspection of Eq. (19), it may be noted that these models look quite similar. One of the major differences among these models is how to take consideration of thermal accommodation coefficients at both plates. In our model, the thermal accommodation coefficients at both plates are used to calculate the overall thermal accommodation coefficient  $\alpha$ , whereas they are assumed to be complete ( $\alpha=1$ ) in Ju’s model or exactly the same ( $\alpha_1=\alpha_2=\alpha_E$ ) in Zhang’s model. However, these assumptions are normally not accurate at the real head-disk interface.

Figure 4 shows the conductive heat flux as a function of the inverse Knudsen number at various  $\alpha$  values. The DSMC simulation results are also quoted in this figure for easy comparison.

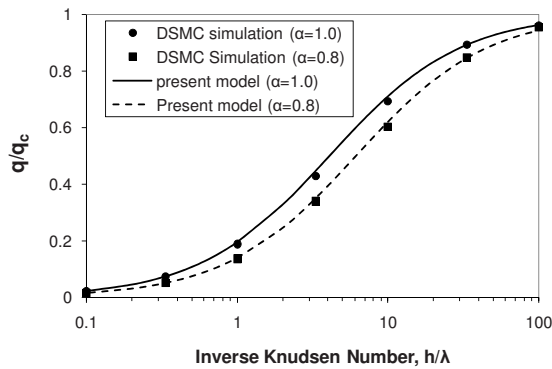


FIG. 4. Conductive heat flux associated with Couette flows as a function of inverse Knudsen Number for various  $\alpha$  values. The heat flux is normalized by the continuum value. The circles and squares correspond to the numerical data obtained from the direct simulation Monte Carlo (DSMC) method. The gas temperature  $T=273$  K and gas pressure  $p=1$  atm.

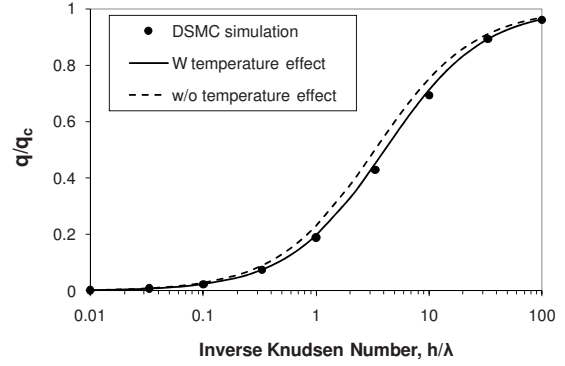


FIG. 5. Conductive heat flux as a function of inverse Knudsen Number. The dashed line corresponds to the simulation results from the previous models without considering temperature effect. The solid line represents the numerical data based on the present model.

It is found that the prediction from our heat conduction model is in good agreement with the DSMC simulation results and thus our model can be well validated. It is also found that as  $\alpha$  value increases, the normalized heat flux  $q/q_c$  increases at the same Knudsen number. This is mainly caused by the stronger interactions between the molecules and the boundaries which enhance the contribution from the continuum heat flux at a big  $\alpha$  value.

Another major difference between our model and previous ones is how to consider the mean free path and the temperature effects at the head-disk interface. Previous models only used the hard sphere (HS) model to calculate the mean free path of a gas without considering its temperature effects. Although the HS model is widely used for its simplicity, it is not realistic because under normal conditions, the effective cross section decreases as the translational energy increases. The rate of decrease is directly related to the change in the coefficient of viscosity with temperature. In HS model, the viscosity coefficient is proportional to the square root of the temperature, which is not characteristic of real gases [19]. Therefore, we proposed a generalized formulation [24] for the mean free path, which incorporates various molecular dynamics models and consider temperature effects

$$\frac{\lambda}{\lambda_0} = \xi \left( \frac{T}{T_0} \right)^{\omega+0.5} \frac{p_0}{p}, \quad (20)$$

where  $\lambda_0$  is the mean free path of air at atmospheric pressure  $p_0$  and reference temperature  $T_0$ ,  $\xi$  is a factor to describe a generalized mean free path for various molecular dynamic models, which is unity for the HS model, and  $\omega$  is temperature exponent of the coefficient of viscosity, which is 0.7 for air [19].

The temperature effect of mean free path on the conductive heat flux is presented in Fig. 5 as a function of inverse Knudsen number. The DSMC simulation results are also quoted in this figure. We can see clearly that the old models overestimate the heat flux between the plates since it does not consider the temperature effect of mean free path, which will decrease the collisions and heat transfer between the air molecules and boundaries as air temperature increases. Therefore, we conclude that temperature effect should be

considered in the simulation model. This is especially important for the disk drives because they always need to operate in a wide temperature range.

### C. Viscous dissipation

We now compare our viscous dissipation term as shown in Eq. (17) with the ones from the previous models. In Zhang's and Ju's models, the viscous dissipation terms are written as

$$\text{Zhang's model: } q_{\text{viscous}} = \frac{\mu U^2 h}{2(h + 2a\lambda)^2} \quad (21)$$

$$\text{Ju's model: } q_{\text{viscous}} = \frac{1}{8} \rho U^2 \left( \frac{8RT}{\pi} \right)^{1/2} \frac{1}{1 + h/2\lambda}. \quad (22)$$

By comparing these expressions, we can see that our model has similar format with Ju's model, except that the effect of the momentum accommodation coefficient was not considered in Ju's model. Compared with Zhang's model, however, it is found that the viscous dissipation term contributed by Couette flow is totally different from our model. Figure 6 compares viscous dissipation among various models as a function of the inverse Knudsen number. The DSMC simulation results are also quoted in this figure. It is found that our prediction agrees well with the DSMC simulation results, but deviates significantly from that of Zhang's model, especially in highly rarefied-flow regime. This is because Zhang's model, which is based on the slip flow theory, assumes that the collisions between molecules are dominant mechanism of viscous dissipation. This assumption is reasonable in continuum and slip flow regimes but will be broken down in transition and free-molecule flow regimes due to the fact that collisions between molecules and boundaries, instead of intermolecular collisions, should be dominant factor in these regimes. It is also found from Fig. 6 that the viscous dissipation increases significantly with  $\sigma$  value for the reason that the stronger interactions between the molecules and the boundaries at high  $\sigma$  value increase the shear stress and further viscous dissipation between two plates. Therefore, we can conclude that momentum accommodation

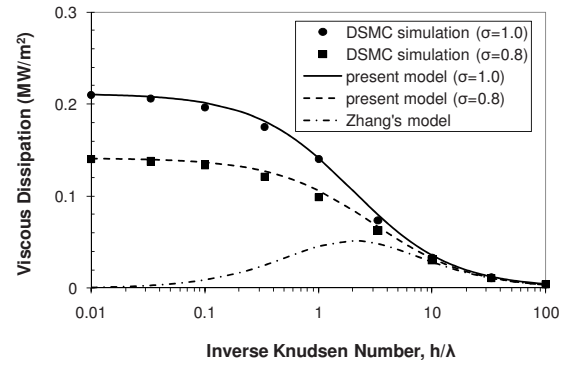


FIG. 6. Viscous dissipation associated with Couette flows as a function of the inverse Knudsen number. The circles and squares correspond to the numerical data obtained from DSMC method. The speed of the moving plate  $U=50$  m/s, the gas temperature  $T=273$  K, and gas density  $\rho=1.78$  kg m<sup>-3</sup>.

coefficient is a very important parameter to determine the viscous dissipation in Couette flow, which should be included in the model to improve simulation accuracy.

### IV. CONCLUSION

A heat transfer model is derived by approximating the heat transfer in the slip and transition regimes as an intermediate function of the asymptotic processes of continuum heat transfer and free molecular heat transfer. By using the Knudsen number to weigh the contributions of two heat fluxes, this model, which is valid for arbitrary Knudsen numbers, is capable to solve the rarefied-gas heat conduction and viscous dissipation in micro/nanoscale Couette flows.

The simulation results based on this model show good agreement with our numerical data obtained from DSMC method. Compared with previous heat transfer models, this model considers many important features at the head-disk interface, such as temperature effects in the disk drive, thermal and momentum interactions on the slider/disk surfaces, and molecular collisions between the air molecules and the solid boundaries. Therefore, this model is expected to provide more accurate prediction of heat conduction and viscous dissipation at the head-disk interface of hard disk drives.

- 
- [1] D. E. Kataoka and S. M. Troian, *Nature (London)* **402**, 794 (1999).
  - [2] N. Koumura, R. W. J. Zijlstra, R. A. van Delden, N. Harada, and B. L. Feringa, *Nature (London)* **401**, 152 (1999).
  - [3] W. Peng, Y. T. Hsia, K. Sendur, and T. McDaniel, *Tribol. Int.* **38**, 588 (2005).
  - [4] B. Liu, S. K. Yu, W. D. Zhou, C. H. Wong, and W. Hua, *IEEE Trans. Magn.* **44**, 145 (2008).
  - [5] S. Fukui and R. Kaneko, *ASME J. Tribol.* **110**, 253 (1988).
  - [6] G. Karniadakis, A. Beskok, and N. Aluru, *Microflows and Nanoflows: Fundamentals and Simulation* (Springer, New York, 2005).
  - [7] B. Liu, S. K. Yu, M. S. Zhang, L. Gonzaga, H. Li, J. Liu, and Y. S. Ma, *IEEE Trans. Magn.* **43**, 715 (2007).
  - [8] D. K. Bhattacharya and G. C. Lie, *Phys. Rev. Lett.* **62**, 897 (1989).
  - [9] P. A. Thompson and S. M. Troian, *Nature (London)* **389**, 360 (1997).
  - [10] B. Cao, M. Chen, and Z. Guo, *Appl. Phys. Lett.* **86**, 091905 (2005).
  - [11] M. Wang and Z. Li, *Phys. Rev. E* **68**, 046704 (2003).
  - [12] W. W. Liou and Y. Fang, *J. Microelectromech. Syst.* **10**, 274 (2001).
  - [13] S. Zhang and D. B. Bogy, *Int. J. Heat Mass Transfer* **42**, 1791

- (1999).
- [14] Y. S. Ju, ASME J. Heat Transfer **122**, 817 (2000).
- [15] Y. S. Ju, IEEE Trans. Magn. **41**, 4443 (2005).
- [16] J. Y. Juang and D. B. Bogy, ASME J. Tribol. **129**, 570 (2007).
- [17] A. Beskok and G. E. Karniadakis, J. Thermophys. Heat Transfer **8**, 647 (1994).
- [18] S. Shen and G. Chen, J. Appl. Phys. **103**, 054304 (2008).
- [19] G. A. Bird, *Molecular Gas Dynamics and The Direct Simulation of Gas Flows* (Oxford University Press, New York, 1994).
- [20] M. Calvert and J. Baker, J. Thermophys. Heat Transfer **12**, 138 (1998).
- [21] G. S. Springer, in *Advances in Heat Transfer*, edited by J. P. Hartnett and T. F. Irvine (Academic, New York, 1971).
- [22] C. L. Tien and G. R. Cunnington, in *Advances in Heat Transfer*, edited by J. P. Hartnett and T. F. Irvine (Academic, New York, 1973).
- [23] M. A. Gallis, J. R. Torczynski, D. J. Rader, M. Tij, and A. Santos, Phys. Fluids **18**, 017104 (2006).
- [24] W. D. Zhou, B. Liu, S. K. Yu, W. Hua, and C. H. Wong, Appl. Phys. Lett. **92**, 043109 (2008).